doi:10.3772/j.issn.1006-6748.2022.03.012

Analysis of force and leakage in water hydraulic motor's piston pairs①

WANG Zhiqiang(王志强)②[*,**], DAI Zejun[*], LI Xinglin[***], HE Wen[**], GAO Dianrong[****]
([*]School of Mechanical Engineering, Hangzhou Dianzi University, Hangzhou 310018, P. R. China)
([**]School of Mechanical Engineering, Zhejiang University, Hangzhou 310058, P. R. China)
([***]Post-Doctoral Research Center, Hangzhou Bearing Test&Research Center Co. Ltd., Hangzhou 310022, P. R. China)
([****]School of Mechanical Engineering, Yanshan University, Qinhuangdao 066004, P. R. China)

Abstract

The positive pressure between pistonwall and piston hole of inner curve water hydraulic motor's piston pairs is analyzed. The flow field of the piston pairs is numerically calculated and analyzed by the use of computational fluid dynamics method. The pressure and velocity distribution of flow field at different clearance is analyzed in the paper. The results show that when the clearance is 4 – 8 μm, with the increase of clearance, the negative pressure and the velocity of piston chamber decrease significantly, the velocity and leakage flow of the clearance increase. However, when the clearance is 10 μm, the negative pressure and the velocity of plunger chamber increase suddenly. By comprehensive analysis, the cylinder annular clearance should be controlled to be near 8 μm.

Key words: water hydraulic motor, piston pairs, clearance, leakage flow, numerical simulation

0 Introduction

In recent years, with the attention increasingly given to environmental pollution, water will become the most popular pressure medium instead of oil. So water hydraulic motor will have a wide developmental foreground as the execute component of hydraulic system. However, the special physical and chemical properties of water will bring a lot of problems in the research. Leakage is one of the major problems of them. In order to reduce the leakage flow and increase the volumetric efficiency of water hydraulic motor, international scholars make lots of work to research these problems. Friction measurement of water-based slippers was presented by Li and Hooke[1] of University of Birmingham in 1991. They found that the measured values are consistent with the clearances predicted using the analysis developed for oil-based slippers. The influence of piston clearance on leakage flow and torque of piston pair was analyzed, and the variation of leakage flow and torque of piston pair under different slot forms of piston was studied by Kumar et al.[2]. Lu et al.[3] studied the influence of rotating speed on the position and leakage of piston pair under high speed and high pressure. Wang[4] used the Matlab simulation analysis to research the influence of different piston cylinder bore diameter and different pressure on the leakage of piston pair. Meshkov et al.[5] studied the stress distribution of the piston in different contact states, and identified the most critical area of high stress.

Liu et al.[6] researched the leakage characteristics of water hydraulic piston pairs with multiple damping holes on the circumference of the piston. Ivantysynova and Baker[7] researched the influence of piston cylinder clearance shape on power loss, leakage and viscous friction, and predicted the pressure field and velocity field in the lubricating oil film. Schenk et al.[8] studied the pressure of piston pairs with different instantaneous displacement by computer simulation technology. Hu et al.[9] established an adaptive eccentric model to research the water film pressure distribution and leakage flow of piston pair. The leaking flow field of the piston sector considering the high press and high velocity were researched. Xu et al.[10] studied the effects of load pressure, inclined angle of swash plate and piston pair clearance on the performance of piston pairs by virtual prototyping techniques. Luo et al.[11] investigated the relationship between the leakage flow of piston and the angle of cylinder bore, then determined the clearance which made the minimum leakage between piston and cylinder bore.

Although, there have been many studies on force

① Supported by the National Natural Science Foundation of China (No. 51505111), China Postdoctoral Science Foundation (No. 2020M681844) and Zhejiang Province Postdoctoral Science Foundation (No. ZJ2020043).
② To whom correspondence should be addressed. E-mail: wzq78452501@163.com.
Received on Sep. 13, 2021

and leakage, they mainly focus on the study under oil lubrication. Limited information is available on the effect of different surface and geometries on flow characteristics between the friction pairs of low speed high torque hydraulic motor under seawater lubrication. To study the force and leakage properties of water hydraulic motor with ten piston pairs under seawater lubrication, the pressure and velocity distribution of flow field at different clearance were simulated by computational fluid dynamics method.

1 Structure features

1.1 Working principle

In this paper, the water hydraulic motor adopts the end face flow distribution mode. The structure of the water hydraulic motor is shown in Fig. 1(a). The port block is embedded in the rear end cover, the left flow channel in the port block is connected with the inlet and outlet of the rear end cover, and the right flow channel is connected with the replaceable friction plate. The right end face of the friction plate is attached to the rotor, which completes the suction and drainage action of the piston by cooperating with the rotation of the rotor.

The distribution and structure of the piston modules in the rotor body of the water hydraulic motor are shown in Fig. 1(b). The piston modules (roller and piston) are uniformly distributed circumferential in the ten piston holes of the rotor body. The pressure water in the flow channel of the rotor acts on the bottom of the piston, making the piston modules close to the inner curved surface of the stator, and at the same time, the modules are subjected to the reaction force from the stator. The tangential component force of the reaction force is transferred to the piston to form a unilateral pressure on the rotor[12], so that the water hydraulic motor turns.

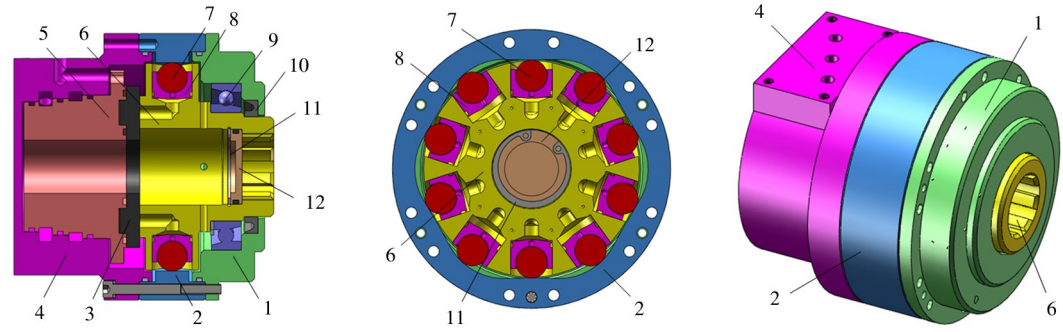

(a) Section drawn of water motor (b) Distribution of piston pairs (c) Outline drawing of water hydraulic motor

1-Front end cap, 2-Stator, 3-Replaceable friction plate, 4-Rear end cap, 5-Port block, 6-Rotor, 7-Roller, 8-Piston, 9-Bearing, 10-Rubber sealing, 11-Circlip, 12-Baffle

Fig. 1 Structure of internal curve type water hydraulic motor

To ensure the movement of the piston, it is necessary to ensure that there is a certain annular clearance between the piston and the piston hole. If the clearance is too big, the leakage of the water hydraulic motor will be greatly increased[13-15]. However, if the clearance is too small, it will be difficult to form a lubricating water film, making a direct contact between the piston and the rotor body which averts the wear and vibration[15-17]. Therefore, the piston pair clearance has an important effect on the performance of water hydraulic motor.

1.2 Materials and specimens

In order to explore the influence of force and leakage on the flow performance of the piston pairs better, the research was carried out on the basis of selecting the optimum matching material. The piston material is made of 316L stainless steel. The steel, which has excellent pitting corrosion resistance and could be safely used in halogen ion environment such as Chloride ion, is usually used in marine environment. The rotor is made of carbon-fifiber-reinforced polyetheretherketone (CFRPEEK), with low friction coefficient, excellent mechanical and corrosion resistance, and can be used in marine environment. The polyetheretherketone(PEEK) of CFRPEEK is white powder with average particle size of 10 μm and density of 1.32 g/cm^3. The reinforcements are short-cut carbon fibers with diameter of 7 μm, density of 1.75 g/cm^3, tensile strength of 3.5 GPa and tensile modulus of 228 GPa.

2 Force analysis of piston pairs

In order to study the friction of piston pair, the

force magnitude of friction can not be ignored[18-20]. For convenience of analysis and calculation, it is assumed that there is no clearance between piston wall and piston hole, and the force of the piston pair is ignored, such as the gravity of the piston pair and the impact force caused by the nonsteady flow in the piston cavity[20-22]. The force on the piston pair is shown in Fig. 2. Suppose that the water supply pressure at the bottom of the piston is N_p and the pressure on the roller reacted by the inner curved surface of stator is N.

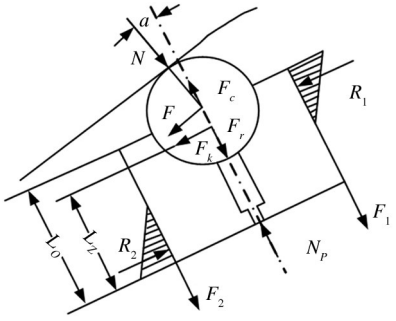

Fig. 2 Force diagram of the piston pairs

Let F be the moment of couple which equivalents to the center of the roller caused by friction, so there is

$$F = \frac{k}{R} \cdot N \tag{1}$$

where k is rolling friction coefficient, R is the radius of the roller.

Supposing the positive pressure on the piston wall and hole are R_1 and R_2, and their corresponding frictions are F_1 and F_2, there are

$$F_1 = fR_1 \tag{2}$$

$$F_2 = fR_2 \tag{3}$$

where f is the friction coefficient between piston wall and piston hole.

Supposing the inertia force caused by the radial acceleration of the piston pair is F_r, there is

$$F_r = ma \tag{4}$$

where m is the mass of the piston module.

Supposing the centrifugal force of the piston pair is F_c, there is

$$F_c = m\omega^2\rho \tag{5}$$

where ω is the angular velocity of the rotor body.

Supposing the inertial force caused by Coriolis acceleration is F_k, there is

$$F_k = 2m\omega v \tag{6}$$

where v is velocity of relative movement between piston wall and piston hole.

To calculate R_1 and R_2, the positive pressure on piston wall and piston hole, supposing the length of R_1 and R_2 acting on the piston wall are L_1 and L_2, and supposing the stresses of piston due to elastic deformation are δ' and δ'', there are

$$R_1 = \frac{1}{2}\delta' L_1 d \tag{7}$$

$$R_2 = \frac{1}{2}\delta'' L_2 d \tag{8}$$

The force between piston wall and piston hole can be further decomposed by the uniformly distributed force along the contact length (δ_N) and the force of two congruent triangles on the centrosymmetric distribution of the contact length (δ_M). The Fig. 3 shows that δ_M is used to balance the torque introduced by δ_N.

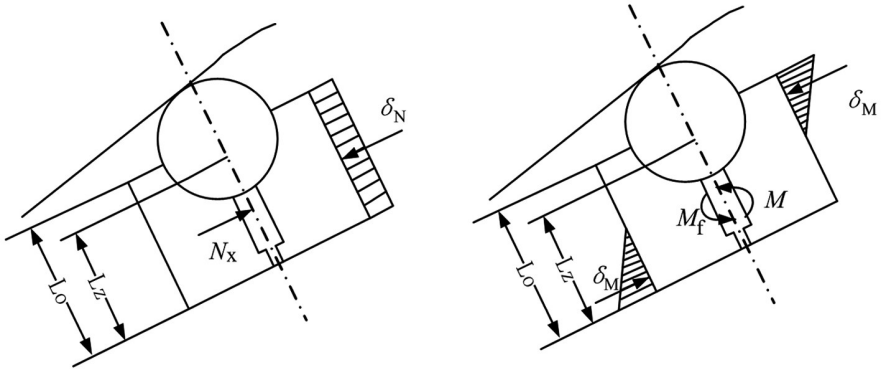

Fig. 3 Stress decomposition diagram of piston pair

So δ' and δ'' can be further rewritten as

$$\delta' = \delta_M + \delta_N \tag{9}$$

$$\delta'' = \delta_M - \delta_N \tag{10}$$

By using the force N, F, F_k involved in Fig. 3, the expressions of tangential force (N_x) and equivalent torque (M) of the piston pair can be derived according to the torque equilibrium equation and the force equilibrium equation. So there are

$$N_x = N \cdot \sin\alpha - F \cdot \cos\alpha - F_k \tag{11}$$

$$M = (N \cdot \sin\alpha - F \cdot \cos\alpha - F_k)(L_o - \frac{L}{2}) - F_k(L_z - \frac{L}{2}) \tag{12}$$

where L_o is the distance from the center of the roller to

the bottom of piston; L is the contact length between piston wall and piston hole; L_z is the distance from the centroid of the piston module to the bottom of piston.

The resultant positive press stress corresponding to N_x is δ_N, which can be derived as

$$\delta_N = \frac{N_x}{L \cdot d} = \frac{N \cdot \sin\alpha - F \cdot \cos\alpha - F_k}{L \cdot d} \tag{13}$$

Defining coefficient A and B as specific expressions as

$$A = \frac{\sin\alpha - \frac{k}{R} \cdot \cos\alpha}{L \cdot d}; \quad B = \frac{F_k}{L \cdot d}$$

So δ_N can be further rewritten as

$$\delta_N = AN - B \tag{14}$$

The friction F_f between piston wall and piston hole caused by the resultant force N_x is calculated as follows.

$$F_f = f \cdot N_x \tag{15}$$

And the moment M_f produced by F_f to the center of the roller is expressed as follows.

$$M_f = F_f \cdot \frac{d}{2} = f \cdot N_x \cdot \frac{d}{2} \tag{16}$$

From the above formulas, the expression of resultant moment M_Σ which acts on the contact length between piston wall and piston hole is as follows.

$$M_\Sigma = M + M_f \tag{17}$$

The positive stress δ_M between piston and the piston hole acted by resultant moment M_Σ can be expressed as

$$\begin{aligned}\delta_M &= \frac{6 \cdot M_\Sigma}{L^2 \cdot d} \\ &= \frac{6}{L^2 \cdot d} \cdot \left[(N \cdot \sin\alpha - F \cdot \cos\alpha)(L_o - \frac{L}{2}) \right. \\ &\quad \left. - F_k(L_z - \frac{L}{2}) + f \cdot N_x \cdot \frac{d}{2} \right] \\ &= \frac{6}{L^2 \cdot d} \cdot \left[\left(N \cdot \sin\alpha - \frac{k}{R} \cdot \cos\alpha\right)(L_o - \frac{L}{2} + \frac{fd}{2}) \right. \\ &\quad \left. - F_k(L_z - \frac{L}{2} + \frac{fd}{2}) \right]\end{aligned} \tag{18}$$

Defining coefficient C and D as specific expressions as

$$C = \frac{6}{L^2 \cdot d} \cdot (\sin\alpha - \frac{k}{R} \cdot \cos\alpha)(L_o - \frac{L}{2} + \frac{fd}{2});$$

$$D = \frac{6}{L^2 \cdot d} \cdot F_k \cdot (L_z - \frac{L}{2} + \frac{fd}{2})$$

So δ_M can be further rewritten as

$$\delta_M = CN - D \tag{19}$$

Due to the stress triangles distributed on both sides of the piston, δ' and δ'' are similar triangles, there is

$$\frac{\delta'}{\delta''} = \frac{L_1}{L_2} \tag{20}$$

Because the contact length L is the sum of L_1 (action length of δ') and L_2 (action length of δ''), then combining Eq. (20) with Eq. (10) and Eq. (11), there are

$$L_1 = \frac{\delta_M + \delta_N}{2\delta_M} \cdot L \tag{21}$$

$$L_1 = \frac{\delta_M - \delta_N}{2\delta_M} \cdot L \tag{22}$$

Substituting Eq. (10), Eq. (11), Eq. (20) and Eq. (21) into Eq. (7) and Eq. (8), the further expressions of positive pressure R_1 and R_2 between piston wall and piston hole can be obtained as

$$\begin{aligned}R_1 &= \frac{1}{2}\delta' L_1 d = \frac{1}{2} \cdot (\delta_M + \delta_N)\left(\frac{\delta_M + \delta_N}{2\delta_M} \cdot L\right)d \\ &= \frac{Ld}{4}\frac{(\delta_M + \delta_N)^2}{\delta_M}\end{aligned} \tag{23}$$

$$\begin{aligned}R_2 &= \frac{1}{2}\delta'' L_2 d = \frac{1}{2} \cdot (\delta_M - \delta_N)\left(\frac{\delta_M - \delta_N}{2\delta_M} \cdot L\right)d \\ &= \frac{Ld}{4}\frac{(\delta_M - \delta_N)^2}{\delta_M}\end{aligned} \tag{24}$$

According to the specific structure size of the hydraulic motor, Fig. 4 shows the relationship between pressure angle α and the positive pressure R_1 and R_2 when the motor speed is 1500 r/min, where α is 0 – 30 °, R_1 and R_2 are 0 – 2500 N.

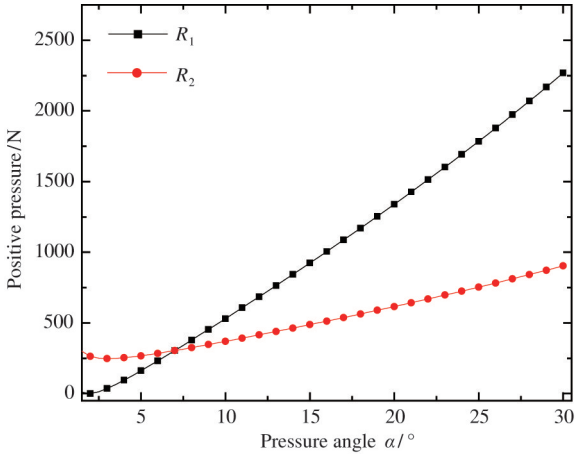

Fig. 4 The change of positive pressure with pressure angle

From Fig. 4, it can be seen that the positive pressure R_1 and R_2 will both increase with the increase of pressure angle α. The friction between the piston wall and piston hole will increase with the positive pressure R_1 and R_2, resulting in the decrease of the width of cylinder annular clearance and its leakage flow.

3 Leakage flow analysis of piston pairs

Fig. 5 shows a picture of concentric clearance of piston and rotor. Setting the diameter of the piston as d, clearance as h, $h << d$, then the annular clearance expanded along the length direction is considered as the same as a plain plate clearance. So the flow rate equation in concentric annular orifice can be obtained as[23-25]

$$Q = \frac{\pi d h^3 \Delta p}{12 \mu L} \tag{25}$$

where πd is circumference of piston, which is the same as the width of plain plate clearance, $d = 20$ mm; Δp is a differential pressure of clearance, 10 MPa; L is the length of clearance, 13.15 mm; μ is kinetic viscosity of fluids, $\mu = 1.005 \times 10^{-3}$ pa · s for water, $\mu = 44.2 \times 10^{-3}$ Pa · s for hydraulic oil.

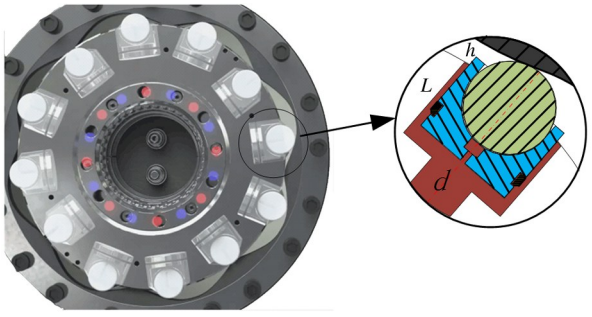

Fig. 5 The clearance of piston and rotor

Substituting available data into Eq. (25), the leakage flow of cylinder annular clearance of pistons and rotor can be got, as shown in Table 1. In those two cases, the change of leakage flow with clearance is shown in Fig. 6.

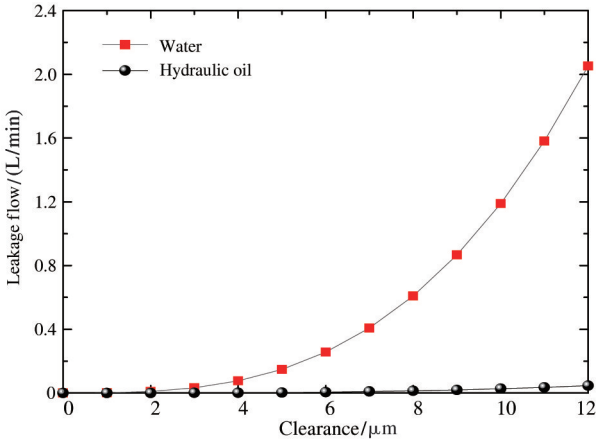

Fig. 6 The change of leakage flow with clearance

Fig. 6 shows the change of leakage flow with clearance between pistons and rotor when the medium is water or hydraulic oil. From Fig. 6, it can be seen that the leakage flow will increase significantly with the increase of clearance when the medium is water. Table 1 shows the comparison of leakage flow of cylinder annular clearance in different medium. It can be seen from the table, when the medium is water, leakage flow rate is about 40 – 50 times of hydraulic oil with the same clearance. So the cylinder annular clearance of piston pairs should not be too large or it will greatly reduce the volumetric efficiency of water hydraulic motor.

Table 1 The comparison of leakage flow of clearance in different medium

Medium	Clearance/μm	Leakage flow/(L/min)
Water	4	0.0152
	6	0.0513
	8	0.1217
	10	0.2376
	12	0.4105
Hydraulic oil	4	0.0003
	6	0.0012
	8	0.0028
	10	0.0054
	12	0.0093

4 Numerical simulation of flow field of piston

4.1 Geometric modelling and meshing

A geometry model of piston pairs flow channel is established by using computational fluid dynamics (CFD) pre-processing software Gambit. Fig. 7 shows the whole flow channel model. The inlet of model is the bottom of the piston. The outlet of model has two parts: the outlet of cylinder annular clearance (outlet 1) and the interior clearance of piston (outlet 2).

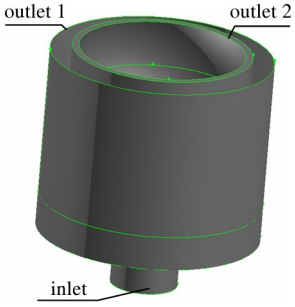

Fig. 7 The flow channel of piston pairs

4.2 Setting of the boundary conditions

In this simulation, water is adopted as the fluid medium. When its operating temperature is 20 ℃, the density is 998.2 kg/m^3 and the kinetic viscosity is $1.005 \times$

10^{-3} Pa · s.

(1) Inlet boundary conditions

The boundary condition in the simulation is given according to the actual working condition. The rated pressure of the motor is 10 MPa, so the given inlet boundary condition is pressure inlet, and the pressure value is 10 MPa.

(2) Outlet boundary conditions

The outlet of the motor is set as the pressure outlet, and the outlet pressure value is 0 MPa. The water film between the piston and roller has leakage, so the side of the water film is set as the pressure outlet, and the pressure of outlet 1 and outlet 2 are 0 MPa.

(3) Wall boundary conditions

Generally, when doing static analysis, the interface between fluid and solid is static by default. For viscous fluid, its viscosity makes it adhere to the solid surface, and the outer most wall should move with the solid surface at the same speed without sliding. Therefore, the wall motion should be taken into account when setting the wall boundary of the motor.

4.3 CFD simulation and analysis

Fig. 8 shows the change of pressure in cylinder annular clearance. From the figure, it can be seen that the pressure distribution remains largely unchanged with the increase of clearance, and the pressure along the axis direction of piston reduces gradually. Besides, the pressure remains constant at the same height.

Fig. 9 shows the pressure contour plot of piston pairs in *YOZ* plane. It can be seen from Fig. 9 that the both sides of damping hole start to have pressure loss, and the pressure loss is constantly moving closer to the inlet of cylinder annular clearance. But the phenomenon will disappear when the clearance is 10 μm. From the pressure contour plot, it was also found that the negative pressure

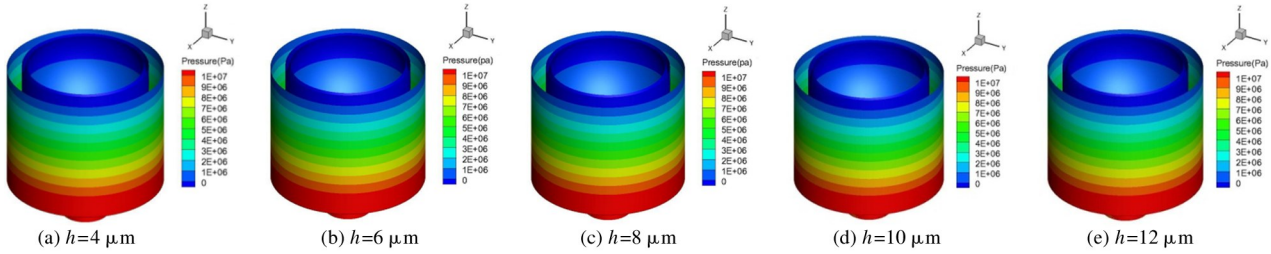

(a) h=4 μm (b) h=6 μm (c) h=8 μm (d) h=10 μm (e) h=12 μm

Fig. 8 The three-dimensional flow field pressure contour

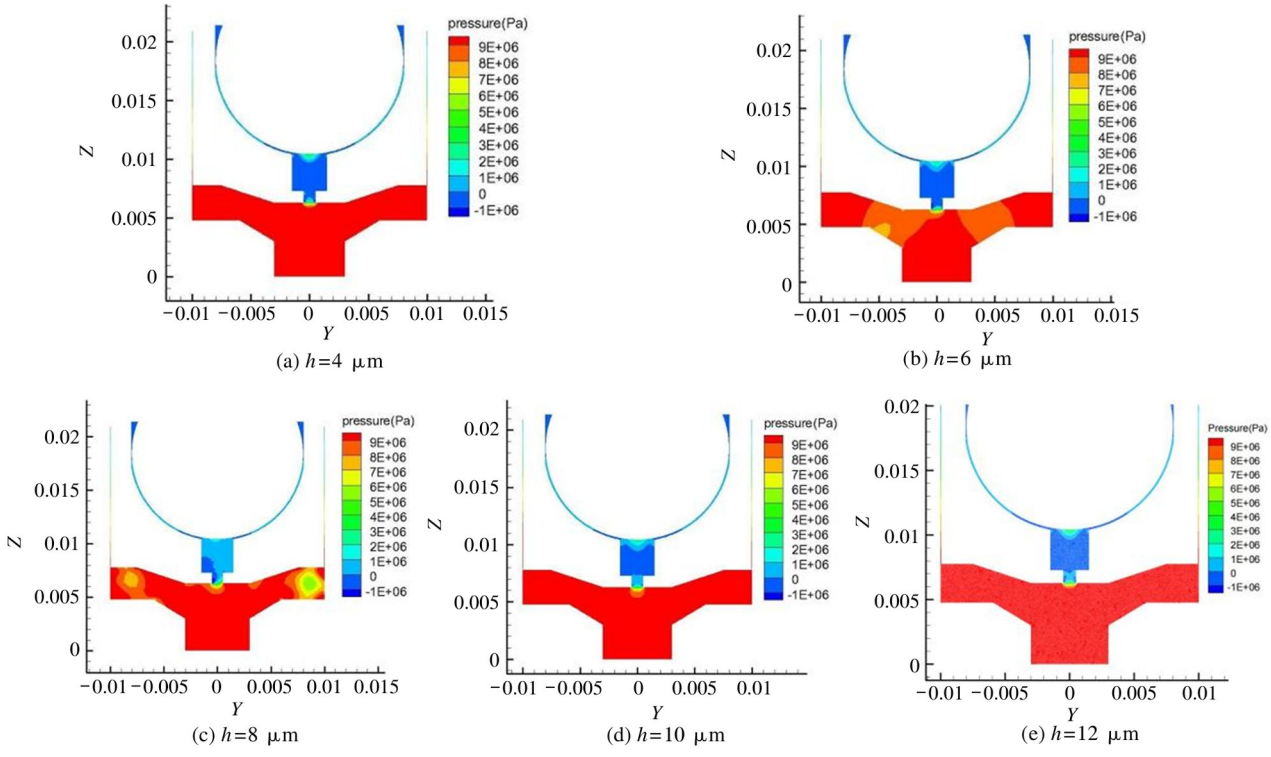

(a) h=4 μm (b) h=6 μm

(c) h=8 μm (d) h=10 μm (e) h=12 μm

Fig. 9 The pressure of piston pairs in *YOZ* plane

of piston chamber decreases with the increase of clearance, but the negative pressure has increasing tendency when the clearance is 10 μm. The higher the negative pressure, the easier it is to case cavitation. So the minimum negative pressure of clearance is the best.

Fig. 10 shows the velocity contour plot of piston pairs in *YOZ* plane. From the velocity contour plot, it can be seen that the location of the maximum flow velocity is at the outlet of damping hole, and the maximum flow velocity of piston chamber decreases significantly with the increase of cylinder annular clearance. However, the maximum flow velocity and the flow velocity in the inlet of cylinder annular clearance will increase suddenly when the clearance is 10 μm. This means the flow velocity of piston chamber is greatly affected by clearance.

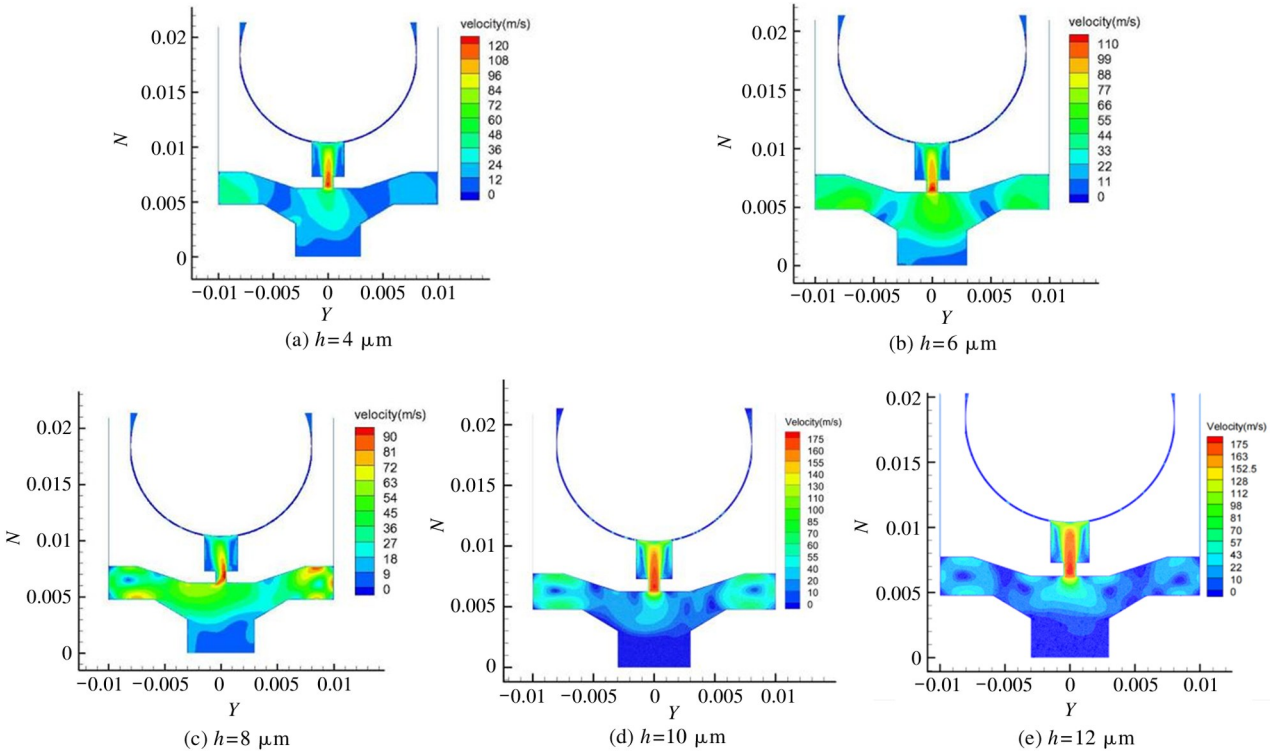

Fig. 10 The velocity of piston pairs in *YOZ* plane

The change curves of pressure and velocity in axis direction of piston at different clearance are shown in Fig. 11 and Fig. 12. Through the pictures, it can be seen that the negative pressure and velocity of piston chamber are the minimum when the clearance is 8 μm. And the maximum negative pressure of piston chamber is obtained when the clearance is 4 μm, the maximum velocity is obtained when the clearance is 10 μm.

Fig. 13 shows the change of velocity with the length of cylinder annular clearance. It can be seen from the figure, in any case, the flow velocity will keep stable at a certain value with the increase of length, but the flow velocity will reduce with the decrease of clearance.

The leakage flow of cylinder annular clearance and interior clearance can also be got by CFD numerical simulation, as shown in Table 2. It can be seen from the table that the leakage flow of cylinder annular clearance goes up with the increase of clearance, and the leakage flow of interior clearance first goes down and then increase with the increase of clearance, and the minimum-leakage flow of interior clearance was obtained when clearance is 8 μm. So the total leakage flow of piston pairs is the minimum when the clearance is 8 μm.

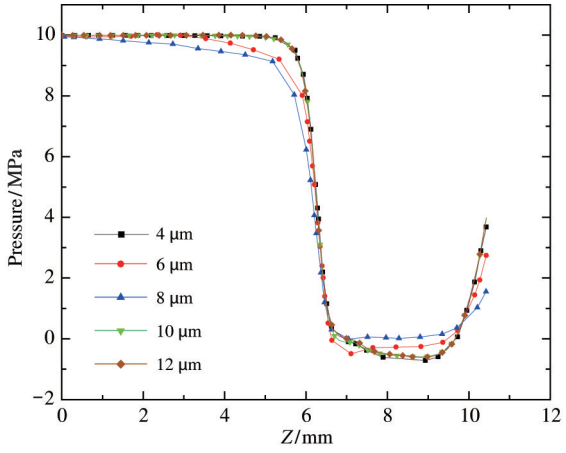

Fig. 11 Pressure in axis direction of piston

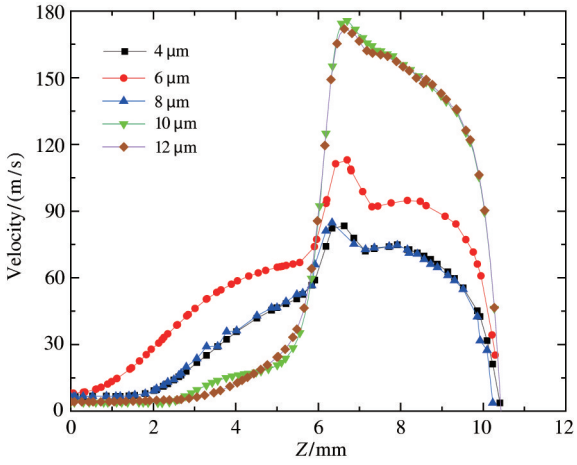

Fig. 12 Velocity in axis direction of piston

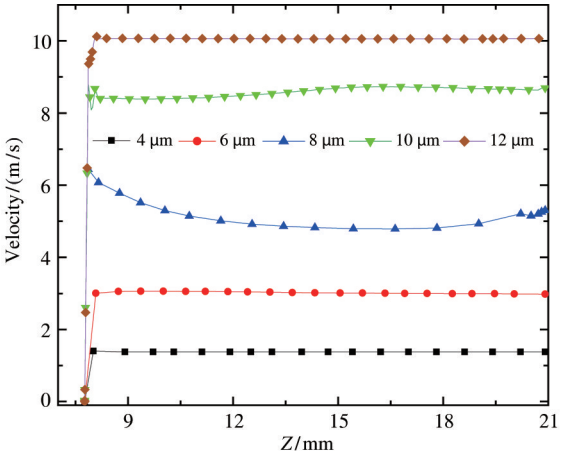

Fig. 13 Velocity curve of cylinder annular clearance

Table 2 The leakage flow of piston pairs

Clearance/μm	Leakage flow of cylinder annular clearance/(L/min)	Leakage flow of interior clearance/(L/min)	Total leakage flow/(L/min)
4	0.0161	4.8253	4.8414
6	0.0523	3.8055	3.8578
8	0.1318	2.9437	3.0755
10	0.2475	4.3727	4.6202
12	0.2906	7.0592	7.3499

5 Conclusion

(1) CFD simulation results show that the pressure of cylinder annular clearance goes down with height in different clearance. Besides, the pressure remains constant at the same height. This means fluid flow obeys the law of laminar flow. Moreover, the results show that with the decrease of clearance, the velocity and leakage flow of the cylinder annular clearance will reduce, and the velocity will keep at a certain value.

(2) By analyzing the pressure contour, velocity contour and total leakage flow of piston pairs, the velocity and the negative pressure of piston chamber are the minimum which will reduce the possibility of occurrence of cavitation and water hammer, and the total leakage flow of piston pairs is also minimum when the clearance is 8 μm. So the clearance should be controlled to be approximate 8 μm.

(3) Under different clearance widths, comparing Table 2 with Table 1 shows that the results of CFD numerical simulation are larger than theoretical calculation. This is because the inertia term is not considered in theoretical calculation, while CFD simulation is more comprehensive. From this point of view, CFD calculation results are more reliable.

References

[1] LI K Y, HOOKE C. A note on the lubrication of composite slippers in water-based axial piston pumps and motors[J]. *Wear*, 1991,147(2): 431-437

[2] KUMAR S, BERGADA J M, WATTON J. Axial piston pump grooved slipper analysis by CFD simulation of three-dimensional NVS equation in cylindrical coordinates[J]. *Computers and Fluids*, 2009, 38(3): 648-663

[3] LU F, XU B, ZHANG J. Simulation analysis of the influence of rotating speed on the posture and leakage of EHA pump's piston pairs[J]. *Chinese Journal of Mechanical Engineering*, 2018,54(20):123-130

[4] WANG W. Analysis on the side leakage amount of the friction between piston and cylinder block in axial piston pump [C] // International Conference on Advanced Design and Manufacturing Engineering, Hangzhou, China, 2014: 336-340

[5] MESHKOV V, SEMENOVA T, KOROCHKINA T. Study of friction effect on the stress-strain state of piston in axial piston pump[J]. *Journal of Friction and Wear*,2000,21(3):59-62

[6] LIU H, KE J, WANG G. Research on the lubrication characteristics of water hydraulic piston friction pairs[J]. *China Mechanical Engineering*, 2007,18(4):434-439

[7] IVANTYSYNOVA M, BAKER J. Power loss in the lubricating gap between cylinder block and valve plate of swash plate type axial piston machines[J]. *International Journal of Fluid Power*,2014,10(2):29-43

[8] SCHENK A, ZECCHI M , IVANTYSYNOVA M. Accurate prediction of axial piston machine's performance through a thermo-elasto-hydrodynamic simulation model[C] // ASME/

Bath Symposium on Fluid Power and Motion Control, Sarasota, USA, 2013: 1-11
[9] HU R, YUAN S, LIU H, et al. Analysis on the leaking flow field of the piston sector considering the high press and high velocity[J]. *Transactions of the Chinese Society for Agricultural Machinery*, 2009, 40(4):221-226
[10] XU B, ZHANG J, YANG H. Simulative analysis of piston-cylinder pair of axial piston pump based on virtual prototype[J]. *Journal of Lanzhou University of Technology*, 2010,36(3):31-37
[11] LUO K, WANG H, DONG X. The Leakage of process analysis of axial piston pump and cylinder hole[J]. *Machinery Design and Manufacture*, 2013(8):133-135
[12] YU Q, WANG D, LI S. Thermal-flow coupling characteristics of hydraulic pump's piston/cylinder interface oil film [J]. *Mechanical and Electrical Engineering Magazine*, 2020,37(7):777-782
[13] LIAO W, CHEN T. Influence of texture size on tribological performance of piston pump seal pair[J]. *Ordnance Material Science and Engineering*, 2020,43(1):72-77
[14] JIAN Q, YAN J, LIN Y. Thermal-flow coupling characteristics of hydraulic pump's piston/cylinder interface oil film [J]. *Mechanical and Electrical Engineering Magazine*, 2020,33(1):70-74
[15] XU Y. Oil Film Theory and Friction Pair Design of Hydraulic Pump and Motor: First Edition[M]. Beijing: China Machine Press,1987: 70-76 (In Chinese)
[16] YANG Z, WU D, CHEN J . The analysis of piston-barrel leakage in a super high pressure water hydraulic piston pump[J]. *Hydromechatronics Engineering*, 2006, 39 (1): 1342-1354
[17] WANG Y, ZHANG W. Summary of fluid power transmission and control technology[J]. *Chinese Journal of Mechanical Engineering*, 2003,39(10):95-99
[18] GAO D, WANG Z. Research progress and development prospect of water hydraulic motors[J]. *Chinese Hydraulics and Pneumatics*, 2014(8):1-8
[19] Danfoss. Water hydraulic pumps and motors[EB/OL]. http://www.danfoss.com: Danfoss, [2021-08-05]
[20] ZAWISTOWSKI T, KLEIBER M. Gap flow simulation methods in high pressure variable displacement axial piston pumps[J]. *Archives of Computational Methods in Engineering*, 2017,24(3):519-542
[21] PELOSI M, IVANTYSYNOVA M. The impact of axial piston machines mechanical parts constraint conditions on the thermo-elastohydrodynamic lubrication analysis of the fluid film interfaces [J]. *International Journal of Fluid Power*, 2013,14(3):35-51
[22] HASHEMI S, FRIEDRICH H, BOBACH L, et al. Validation of a thermal elastohydrodynamic multibody dynamics model of the slipper pad by friction force measurement in the axial piston pump [J]. *Tribology International*, 2017, 115 (5):319-337
[23] KIM Y, HAM Y, PARK S. Energy recovery through awater-hydraulic motor in a small-scale RO desalination system[J]. *Desalination and Water Treatment*, 2010,15:172-177
[24] YANG H, YANG J, ZHOU H. Research on materials of piston and cylinder of water hydraulic pump[J]. *Industrial Lubrication and Tribology*, 2003,55(1):38-43
[25] GAO D, WU X. Engineering Fluid Mechanics[M]. Beijing: China Machine Press, 1999: 118-122 (In Chinese)

WANG Zhiqiang, born in 1984. He received his Ph. D degree from Yanshan University, China, in 2014. He joined School of Mechanical Engineering at Hangzhou Dianzi University in 2014. His current position is an associate professor of the school. From 2017 to 2018, he was invited to University of Southampton as a visiting scholar. His research interests include lubrication mechanism and friction and wear of seawater hydraulic motor.